Biol. Cybern. 88, 395–408 (2003)
DOI 10.1007/s00422-002-0384-4

Biological Cybernetics

Activity dynamics and propagation of synchronous spiking in locally connected random networks

Carsten Mehring[1,*], **Ulrich Hehl**[1,*], **Masayoshi Kubo**[2], **Markus Diesmann**[3], **Ad Aertsen**[1]

[1] Neurobiology and Biophysics, Inst. of Biology III, Albert-Ludwigs-University, Schänzlestr. 1, 79104 Freiburg, Germany
[2] Department of Applied Analysis and Complex Dynamical Systems, Graduate School of Informatics, Kyoto University, Kyoto 606-8501, Japan
[3] Department of Nonlinear Dynamics, Max-Planck Institut für Strömungsforschung, Bunsenstr. 10, 37073 Göttingen, Germany

Received: 28 December 2001 / Accepted in revised form: 26 November 2002 / Published online: 7 April 2003

Abstract. Random network models have been a popular tool for investigating cortical network dynamics. On the scale of roughly a cubic millimeter of cortex, containing about 100,000 neurons, cortical anatomy suggests a more realistic architecture. In this locally connected random network, the connection probability decreases in a Gaussian fashion with the distance between neurons. Here we present three main results from a simulation study of the activity dynamics in such networks. First, for a broad range of parameters these dynamics exhibit a stationary state of asynchronous network activity with irregular single-neuron spiking. This state can be used as a realistic model of ongoing network activity. Parametric dependence of this state and the nature of the network dynamics in other regimes are described. Second, a synchronous excitatory stimulus to a fraction of the neurons results in a strong activity response that easily dominates the network dynamics. And third, due to that activity response an embedding of a divergent-convergent feed-forward subnetwork (as in synfire chains) does not naturally lead to a stable propagation of synchronous activity in the subnetwork; this is in contrast to our earlier findings in isolated subnetworks of that type. Possible mechanisms for stabilizing the interplay of volleys of synchronous spikes and network dynamics by specific learning rules or generalizations of the subnetworks are discussed.

1 Introduction

Investigations of cortical network models face two structural problems. Analytical approaches necessitate a strongly simplified architecture, possibly to the degree that it becomes arguable whether results can still be related to real brains. On the other hand, more realistic computer simulations may obscure underlying mechanisms if the system becomes too complex, and often cannot handle the relevant numbers of neurons and connections due to restrictions in computation time and memory.

In this study, we chose a compromise. To investigate the activity dynamics in the cortical network at the scale of one cubic millimeter, containing on the order of 100,000 neurons, we explored a network model that, we will argue, is more realistic than a random network but simple enough to, in principle, allow for analytical treatment.

The rules we adopted to construct our network topology were derived from statistical neuroanatomy. Recent anatomical results in rat visual cortex (Hellwig 2000) provide a quantitative local connectivity rule: the probability for two pyramidal neurons to share a synapse decreases with distance in a Gaussian fashion, with a space constant of about 0.3 mm. While this rule ignores axonal patches (Amir et al. 1993) and long-range connections (for a new quantitative result see Schüz and Liewald 2001), this does not pose a problem here since the size of the simulated network of about 100,000 neurons coincides with the range governed by local connectivity. For this reason our network layout and connectivity scheme are based on these data, and we describe here the dynamics in such locally connected random networks (LCRNs). The idea of local connectivity is not new (Wilson and Cowan 1973; Amari 1977), and it is well conceivable that mean field theories in the spirit of that work can be extended to include our findings.

Sparsely connected random networks admit states of activity in which the average excitation and inhibition are in equilibrium and the neurons sustain a level of low firing rates (“Balanced Networks”; van Vreeswijk and Sompolinsky 1996; van Vreeswijk and Sompolinsky 1998; Amit and Brunel 1997). A recent analytical study of Brunel (2000) discerned the dynamic states in large networks of integrate-and-fire neurons and classified them by the combination of two properties: a population

Correspondence to: Carsten Mehring
(e-mail: mehring@biologie.uni-freiburg.de,
Tel.: +49-(0)761-203-2786, Fax: +49-(0)761-203-2860)
* *These authors contributed in equal parts.*

activity that ranges from **S**ynchronous to **A**synchronous, and the firing patterns of single neurons ranging from **R**egular to **I**rregular. Hence, four prototype states were named according to the four possible combinations: SR, AR, SI, and AI.

The first question that arises when we make the transition from random to neighborhood coupling in LCRNs is whether these states still exist. In comparison to the study of Brunel (2000), the dynamics of our LCRN are altered not only by the local connectivity, but also by the more realistic modeling of synaptic transmission: we shaped postsynaptic currents (PSCs) as α-functions with a rise and decay time, whereas Brunel (2000) used δ-functions without a rising or decaying phase. The crucial point is to at least achieve a stable stationary asynchronous-irregular (AI) state. This enables us to use the network activity as a more realistic substrate to mimic the different types of ongoing activity than the uncorrelated noise that is commonly applied to model neurons.

It turns out that this AI state is indeed achievable in LCRNs for a wide range of parameters. It thereby provides a useful tool for investigating the propagation of volleys of synchronous spikes in divergent-convergent subnetworks (''Synfire Chains'', Abeles 1991) that are no longer isolated and fed with artificial Poissonian background as in Diesmann et al. (1999). It was even predicted that the connectivity in LCRNs inherently provides for such subnetworks for statistical reasons (Hehl et al. 2001; Hehl 2001). Here we consider whether they are dynamically functional within an LCRN, i.e., whether a volley of synchronous spikes is sustained and propagated in stable fashion.

We addressed this question in two stages. First, we stimulated a fraction of neurons in the network with a single volley of synchronous spikes. The result was devastating, as the network responded with an explosion in activity. A thorough parametrical study of this ''synfire explosion,'' as we called it, demonstrates this to be a general feature of the network.

Since the inherent convergence of the neurons connected to the stimulus is obviously too weak to propagate the spike volley in the presence of a synfire explosion, we modified the LCRN connectivity by explicitly embedding a synfire chain. We found that, depending on the embedding scheme, the ability to propagate synchronous spike volleys varies from barely to not at all, which is in sharp contrast to the isolated case (Diesmann et al. 1999; Gewaltig et al. 2001). In addition, the whole network is strongly affected by the volley; the AI state is not conserved and only reentered after the volley has dissipated.

At least at first glance, this appears to be a severe blow against the synfire hypothesis. Thus, we will suggest modifications of the synfire chain definition to cope with the above-described phenomena.

This study starts with a methods section describing the neuron model, network architecture, and simulation tools. The results section provides quantitative evidence for the claim that an AI state exists in LCRNs. Also, we discuss which other states were observed and how they depend on network parameters. Then we describe the parametric dependence of the synfire explosion and its implications for the functionality of an embedded synfire chain. Finally, in the discussion section, we review the relevance and possible shortcomings of our LCRN concept, evaluate whether the synfire explosion is a general phenomenon independent of this particular network topology, and discuss possible means by which the synfire chain theory may escape this explosion.

2 Methods

2.1 Model neuron

Neurons were modeled as leaky integrate-and-fire neurons with voltage threshold (Tuckwell 1988 and references therein). Model parameter values were chosen consistently with the experimental literature. Whenever the membrane potential crossed the threshold of $\Theta = -50$ mV, a spike was elicited and the neuron reset to its resting potential $U_r = -70$ mV, followed by a refractory period of 2 ms. The membrane time constant was set at $\tau = 10$ ms. Excitatory postsynaptic currents were taken to be α-functions, with a rise time of 0.3 ms and a current peak amplitude that leads to a realistic postsynaptic potential (PSP) with a peak of $J = 0.14$ mV occurring 1.7 ms after the onset. IPSPs had the same shape, but a peak amplitude scaled by a factor g. The dynamics were integrated on a time grid with constant spacing of 0.1 ms (Rotter and Diesmann 1999). Further details are described in Diesmann et al. (2001).

2.2 Network architecture

One source of motivation to study LCRNs was the quantitative anatomical result that the local connection probability of two pyramidal neurons in rat visual cortex as a function of their cell body distance (Hellwig 2000) can be described by a Gaussian with standard deviation $\sigma_n = 0.3$ mm. This holds true for the distance within a cortical layer; the connectivity across layers has a more complicated structure (Krone et al. 1986). Therefore, in addition to wanting to keep matters simple, we decided on a 2D network layout, where the neuron density in layers II/III of approximately 75,000 excitatory neurons per cubic millimeter (Peters et al. 1985) is adapted as if one had taken layers II and III of rat visual cortex and squeezed their total thickness of 0.3 mm (Gabbott and Stewart 1987; Hellwig 2000) into a 2D sheet.

Our simulation capacities restricted us to a network of about 100,000 neurons. With a physiological ratio of about one inhibitory neuron per four excitatory neurons (Braitenberg and Schüz 1998), a choice of a square area with $l = 2$ mm in length contains $0.3\,\mathrm{mm} \times (2\,\mathrm{mm})^2 \times 75,000\,\mathrm{mm}^{-3} = 90,000$ excitatory neurons and, consequently, 22,500 inhibitory neurons. In our simulations, these were positioned on a regular orthogonal grid with

a space constant of 0.007 mm, which is well below the connectivity space constant σ_n.

To avoid the effect that a neuron near the boundary receives less input, the area was folded as a torus. For activity to reach the neuron it originated from, it must cover $l/\sigma_n = 6$ standard deviations. This is a concession to the inevitable constraints of computing resources and enough to minimize short-term reverberations, but it does not suffice to state that there are no boundary effects at all.

To our knowledge, no data are available concerning the distance dependence of the connectivity probability for inhibitory neurons, one reason being their larger variability in cell type. Therefore, we assumed the same Gaussian profile for connections involving inhibitory neurons. The synaptic delay D was set to $D = 1.5$ ms regardless of distance, as signals are fast on this spatial scale.

Figure 1a illustrates the choice of the $K_E = 9,000$ excitatory and the $K_I = 2,250$ inhibitory presynaptic connections per neuron, and the network layout is depicted in Fig. 1b.

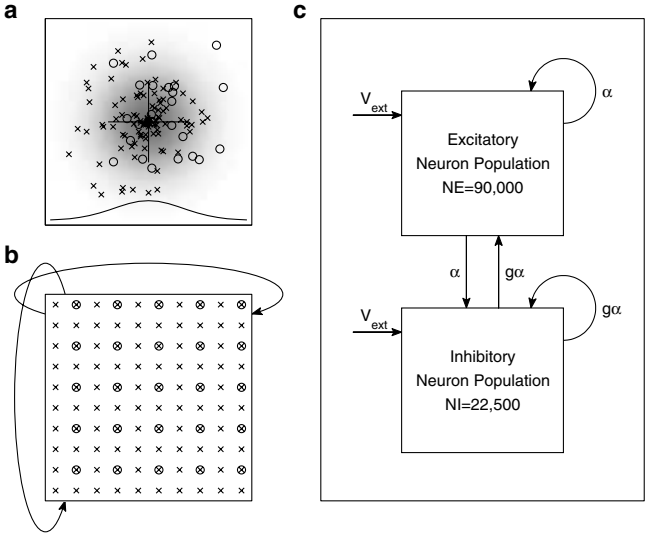

Fig. 1. Locally connected random network (LCRN) architecture. **a** Illustration of connectivity for a sample neuron (location indicated by "+"). Connections are established from $K_E = 9,000$ excitatory (marked as "x") and $K_I = 2,250$ inhibitory ("o") presynaptic neurons, chosen at random with a probability decreasing with distance according to a Gaussian (*gray shading*; *solid curve* shows cross-section profile). **b** Layout of the network. 90,000 excitatory neurons ("x") are arranged on a regular square grid spanning 2×2 mm^2, with 300 neurons along each line at a 6.7μm spacing. 22,500 inhibitory neurons are positioned on every fourth grid point, overlying the excitatory population ("o," plotted on top of the excitatory neuron). The boundaries are connected (*arrows*), leading to a torus-shaped network. **c** Network connectivity. Excitatory and inhibitory neurons each receive input from 11,250 recurrent synapses as described in **a**, here depicted as connections feeding back into the same and projecting to the other population. Additionally, each neuron in both populations receives K_E Poissonian external inputs at a total rate of $K_E \nu_{\text{ext}} \nu_{\text{thr}}$ to represent the part of the embedding network that is not explicitly incorporated. The strength of inhibitory synapses is scaled by a factor g as compared to the excitatory synaptic strength J

The connectivity on a population basis is shown in Fig. 1c, analogous to that of Brunel (2000). Assuming equal mean firing rates of excitatory and inhibitory neurons, the weight g of the inhibitory vs. excitatory PSP naively would range in the order of 4 to obtain a balanced network despite the lower number of inhibitory neurons. Furthermore, each neuron receives a Poissonian external input at a rate $K_E \nu_{\text{ext}} \nu_{\text{thr}}$, reflecting longer-ranged connections from additional K_E excitatory neurons. We express external input by the parameter ν_{ext}, which is the input rate at each external synapse divided by the threshold rate $\nu_{\text{thr}} = (\Theta - U_r)/(\tau J K_E)$, with the various parameters as defined in Sects. 2.1 and 2.2.

2.3 Simulation tools

The computational requirements of the simulations are quite demanding. The simulation software NEST/SYNOD (Diesmann et al. 1995; Diesmann and Gewaltig 2002) had to be extended with the help of the Message Passing Protocol (MPI, Pacheco 1997) to make use of parallel computing. We performed simulations both on clusters of LINUX PCs and on a parallel computer (SGI Origin 2000, Computing Center at University of Freiburg). Still, with ten processing units it takes about 10 min simulation time for 1 s of simulated "brain" time for our network design as described.

3 Results

3.1 Dynamic states of network activity

A sparsely and randomly connected network of excitatory and inhibitory integrate-and-fire neurons exhibits different dynamical states, depending on the inhibition weight g and the external input ν_{ext} (Brunel 2000). We briefly review two characteristics that are used to classify the states and directly apply these to the results of a parameter scan in the (g, ν_{ext}) space for our LCRN.

Synchronicity is defined as a property of the population activity (cf. Brunel 2000): a network state is termed either asynchronous in the case of stationary global activity or synchronous in the case of oscillatory global activity. To quantify the synchronicity and the fluctuations in the network activity, we calculated the coefficient of variation of the population activity as a function of the control parameters g and ν_{ext} (Fig. 2a). Synchronicity is high in three different regions of the parameter space: for very low external inputs ($\nu_{\text{ext}} \leq 0.9$) and ($g \geq 4$), for an intermediate inhibition weight around 4.5 and intermediate to high external inputs ($\nu_{\text{ext}} > 2$), and in the case of dominating excitation ($g < 4$), where synchronicity is always high, independently of the external input.

The regularity of the spike train of a single neuron is measured by the coefficient of variation (CV) of the interspike interval. A low CV reflects more regular spiking, with the extreme of a clocklike pattern for CV

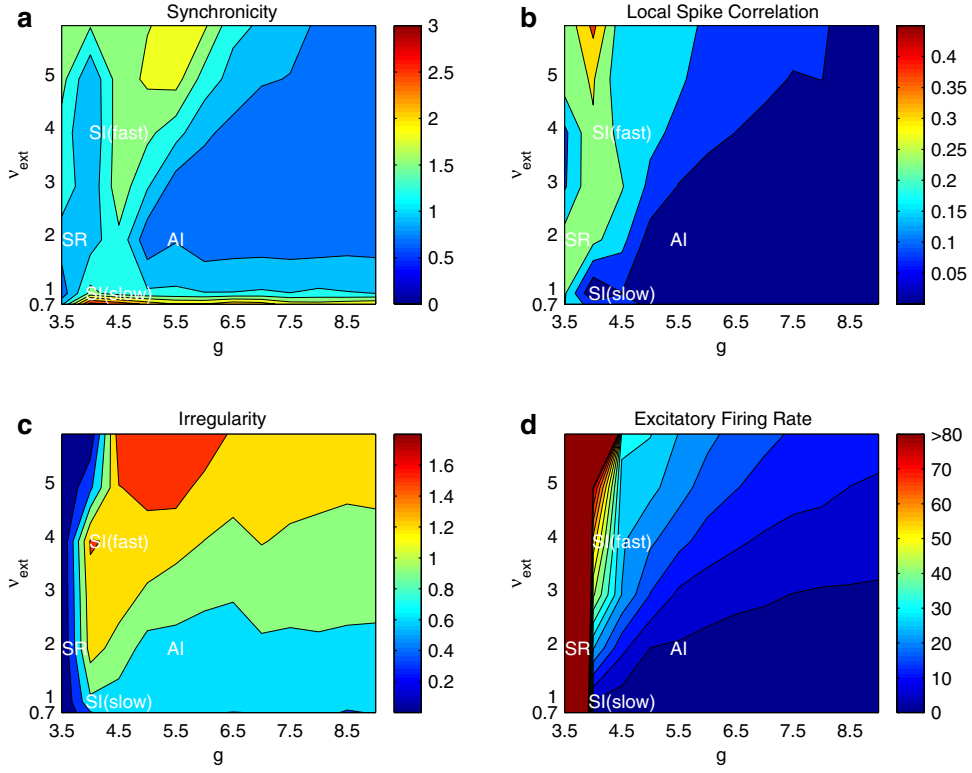

Fig. 2. Phase diagram of dynamic states in LCRN. Subfigures **a–d** show different characteristics of the network dynamics in dependence of the network parameters g and ν_{ext}. The parameter space was sampled on a grid with values of g equal to $3.5, 4.0, \ldots, 9.0$ and values of ν_{ext} equal to $0.7, 0.9, 1.9, \ldots, 5.9$. The values at the grid points were linearly interpolated to obtain the equidistant contour lines shown in the graphs. To guarantee a reliable estimate of the different characteristics, the network was simulated for a period of ten times the average interspike interval. *White text labels* name the regimes of four distinct network states and are placed at parameter values corresponding to the examples shown in Fig. 3. **a** Color-coded synchronicity of the global activity measured by coefficient of variation of the population activity. Contour lines are drawn in steps of 0.3. Three different regimes with high synchronicity, in contrast to one broad asynchronous regime, can be observed. **b** Color-coded sharp spike correlations (± 1 ms) averaged over 1000 neuron pairs with distances between 0.035 mm and 0.140 mm. Generally, spike correlations increase with decreasing inhibition strength and increasing external input. **c** Color-coded coefficient of variation (CV) of the interspike intervals of single neurons with contour lines in steps of 0.3. The CV was calculated by averaging the CVs from 1000 individual neurons. High values were observed for $g \geq 4.5$, whereas neurons fire regularly for low inhibition weight ($g < 4$). **d** Average firing rate of excitatory neurons with contour lines every 5 Hz. For $g \geq 4$, firing rates decrease with increasing inhibition and decreasing external input. For weak inhibition ($g < 4$), neurons fire at their maximum rate

zero. On the other hand, a Poisson process has a CV of 1 as a prototype of "random" behavior. The regularity of the neuronal activity in the network as a function of the control parameters g and ν_{ext} is shown in Fig. 2c. It exhibits two regimes: for $g \geq 4.5$, neurons fire highly irregularly with CVs between 0.5 and 1.8, in contrast to the area of $g < 4$, where neurons exhibit a clocklike firing pattern with CVs near zero. The borderline at $g = 4$ is characterized by decreasing irregularity for high external input.

Taking these two characteristics, synchronicity and regularity, we can now classify four network states, locate their occurrence in the parameter space, and compare them to the states observed in networks with random connectivity and without synaptic current dynamics (Brunel 2000).

In the case of dominating excitation ($g < 4$), the population activity is oscillatory with individual neurons firing regularly; this state is, thus, termed synchronous-regular (SR). Sample spike trains together with the time trace of the population activity for this state are shown in Fig. 3a. This state is similar to the SR state observed in networks with random instead of local connectivity (Brunel 2000).

For intermediate values of the inhibition weight ($4 < g < 6$) and external inputs above ≈ 2, a regime with synchronicity at high oscillation frequencies (around 100 Hz) and irregular firing, named SI (fast), was observed (Fig. 3b). With increasing external input, the parameter regime of this state enlarges to higher values of g (cf. Fig. 2a and Fig. 2c). Remarkably, random networks without synaptic current dynamics do not exhibit strong oscillations in this parameter region. However, a comparable SI state with high oscillation frequencies is found in random networks with strong inhibition and high external input (Brunel 2000). Due to the synaptic current dynamics included in our neuron model, the frequency of the oscillation in this state is determined not only by the synaptic delay D but also by the rise time of the PSP (postsynaptic potential).

Very low external input and $g \geq 4$ leads to oscillatory behavior at low frequencies with individual neurons

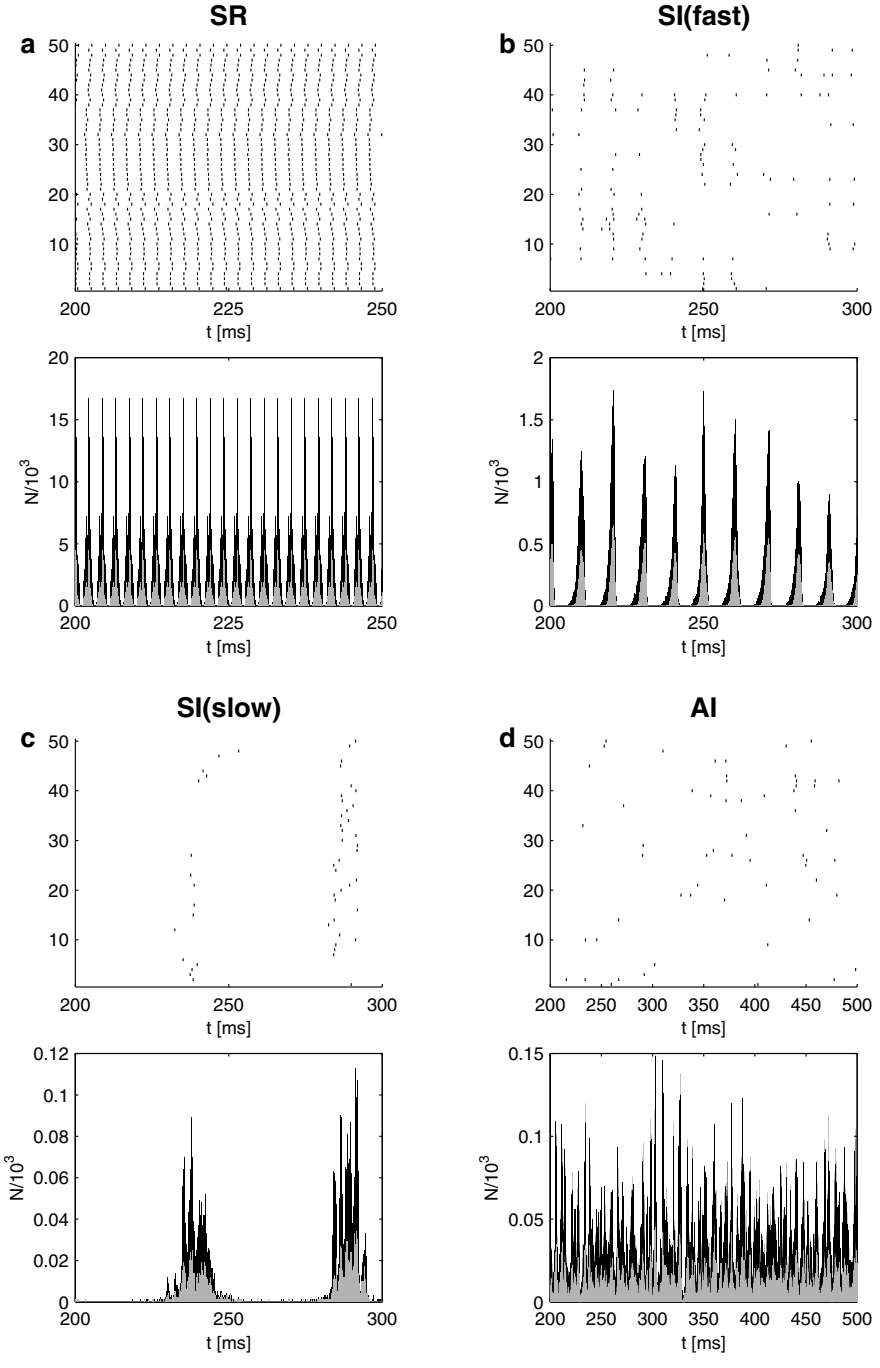

Fig. 3. Examples of network states. Subfigures **a–d** show the population activity (number of neurons firing in bins of 0.1 ms) and sample spike trains for four different states of the network dynamics. The first 200 ms are omitted from the graphs, this period being an upper bound for the time needed by the network to reach its stationary state. The four examples shown correspond to parameter values marked by *white labels* in the phase diagrams of Fig. 2. **a** Synchronous-Regular (SR) with $g = 3.5$, $\nu_{\text{ext}} = 1.9$. The *upper* panel shows sample spike trains of 50 randomly selected excitatory neurons firing clock-like at a rate of almost 500 Hz. The overall population rate of the excitatory neurons (black) and the inhibitory neurons (grey) in the *lower* panel shows a pronounced regular oscillation at the same frequency. **b** Synchronous-Irregular (SI fast) state with $g = 4.5$, $\nu_{\text{ext}} = 3.9$. Same panels as in **a** but different scaling. The population activity is highly oscillatory at around 100 Hz with population bursts of varying size. **c** Synchronous-Irregular (SI slow) state with $g = 4.5$, and $\nu_{\text{ext}} = 0.7$. In contrast to **b**, the frequency of the oscillation is much smaller, and the number of neurons and spikes in a population burst is less than in **b**. As the firing rate is very low in this state (around 1.5 Hz), the *upper* panel shows the spike trains of 50 selected neurons, each of them participating in at least one of the two bursts shown in the graph. **d** Asynchronous-Irregular (AI) state with $g = 5.5$, $\nu_{\text{ext}} = 1.9$. The overall population rate in the lower panel does not exhibit a pronounced oscillation at any one frequency but rather an irregular fluctuating trace

firing irregularly (Fig. 3c). This state corresponds to the state SI (slow) found for similar network parameters g, ν_{ext} in random networks (Brunel 2000).

An asynchronous irregular state (Fig. 3d) is observed for a broad range of inhibition weights and external input strengths. In contrast to networks with random connectivity, the AI state becomes unstable for intermediate values of g (around 4.5) if external inputs are strong enough, but it remains stable for strong inhibition and high external inputs, where random networks exhibit a transition to a fast oscillation. To clarify if an oscillation occurs locally, we measured the sharp spike correlation (± 1 ms) between nearby neurons (0.035 mm – 0.14 mm) as a function of g, ν_{ext} (Fig. 2b). Clearly, local correlations remain low in the whole AI regime, but do not vanish completely. In the AI state, correlations are strongly distance-dependent and decrease more rapidly than the connection probability, as shown in Fig. 4a for the set of network parameters used in Fig. 3d. Local correlations are higher than in random networks, whereas correlations decrease to zero at large distances.

As an additional characteristic of the network activity we computed the average firing rate of the excitatory neurons (Fig. 2d). Two regimes can be clearly distinguished: for values of g smaller than 4, neurons fire almost at their maximum rate (500 Hz) given by their absolute refractory period, independently of the external

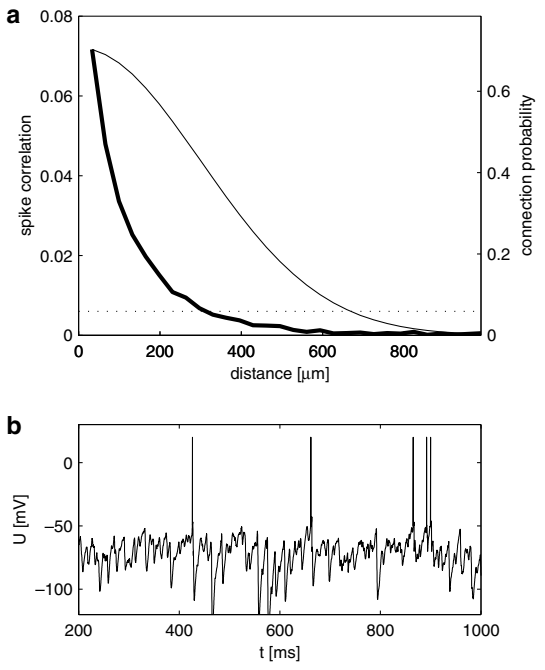

Fig. 4. **a** Average sharp spike correlation (±1 ms) as a function of the distance between neurons (*bold solid line*). Network parameters correspond to an AI state and were chosen as in Fig. 3d. Note that sharp correlations decrease faster than the connection probability (*thin solid line*). In a random network with the same network parameters, correlations are low and not distance dependent (*dotted line*). **b** Variation of the membrane potential of a single excitatory neuron over time illustrates the emergence of the irregular spiking in the AI state

input. For stronger inhibition ($g \geq 4$), the firing rate decreases with increasing inhibition strength and decreasing external input.

We emphasize that, in particular, a network state exists with low firing rate, irregular single-neuron spike patterns, and the absence of overall synchrony in the network (AI; Fig. 3d; an illustrative membrane potential trace of one neuron is shown in Fig. 4b). This is the kind of activity that one typically describes as cortical background activity (e.g., Arieli et al. 1996), and we focus on this AI state for the remainder of this study.

3.2 Impulse response of LCRN: the synfire explosion

What happens if the network is stimulated with a transient volley of synchronous spiking activity? To generate such a transient stimulus, we forced a number of s neurons to emit a spike within a single simulation step, regardless of their membrane potential, and afterwards let their dynamics develop as if the spikes had been elicited by a regular threshold crossing. These s neurons were randomly chosen with a probability decreasing from the center according to a Gaussian with standard deviation σ_s, just as in the selection of presynaptic neurons during network setup. The strength of the spike volley s and its spatial extent σ_s were systematically varied, as shown in Fig. 5a. In view of the torus nature of the network and due to symmetry, the center is distinguished in no other respect than its position on the display.

Figure 5b shows the immediate effect of the stimulus. It is quite obvious that it needs only a moderate number of neurons s to have large effects. We call this response a "synfire explosion," because it shakes the whole network, temporarily forcing it out of the stationary AI state.

An even more severe effect is caused by the inhibition. Simultaneously with the excitatory explosion shown, an inhibitory explosion of essentially the same size and shape is elicited (not shown here). It takes one more synaptic delay for this inhibitory explosion to quench almost all activity in the network. Afterwards, the external input restarts the ongoing activity, and further explosions may develop (Fig. 5c–e).

To better understand this time evolution of the synfire explosion, let us first examine the activity in the transient phase after initialization of the network simulation, where all membrane potential values are at resting value and all currents set to zero (Fig. 6a). There are no spikes traveling, and all neurons are initially affected solely by the external input. Since this Poissonian input represents a large number of external neurons, the network neurons are nearly uniformly driven across threshold to generate a large peak in population rate. Those neurons that spike are all reset to the same resting potential. At first sight, therefore, one would expect a second peak of equal strength sometime later. But the temporal distribution of spikes in the first peak, together with the differences in individual Poisson inputs, starts to disperse the membrane potential distribution. Consequently, the secondary and later peaks ("echoes") gradually become smaller, until they vanish, and the network settles into the stable AI state. Before stimulating the network with a synchronized volley of spiking activity, we always waited until the network had settled into the stable AI state.

We are now in a position to explain the time evolution of the synfire explosion (Fig. 5c–e). After the first activity explosion all neurons are simultaneously reset to the same resting potential. If the explosion is strong enough to locally recruit almost all neurons, these neurons will be subject to the same mechanism that causes the large activity transient at simulation start: the synfire explosion creates echoes as well, and it may take up to three such echoes for the explosion to dissolve.

We can better observe the strength of the explosion and its echoes in a population rate profile (Fig. 6b). All in all, the network needs about 50 ms to recover from a synchronous stimulus of about 100 spikes or more. During this time, the network dynamics are dominated by the stimulus, and the network is temporarily out of balance.

Figure 6c quantitatively evaluates the strength of the synfire explosion, i.e., the total number of spikes within the time window of the first excitatory response. Obviously, a stronger stimulus causes a larger explosion. A larger spatial spread of the stimulus helps to decrease the explosion size, unless it is strong enough to activate the whole network (Fig. 6d).

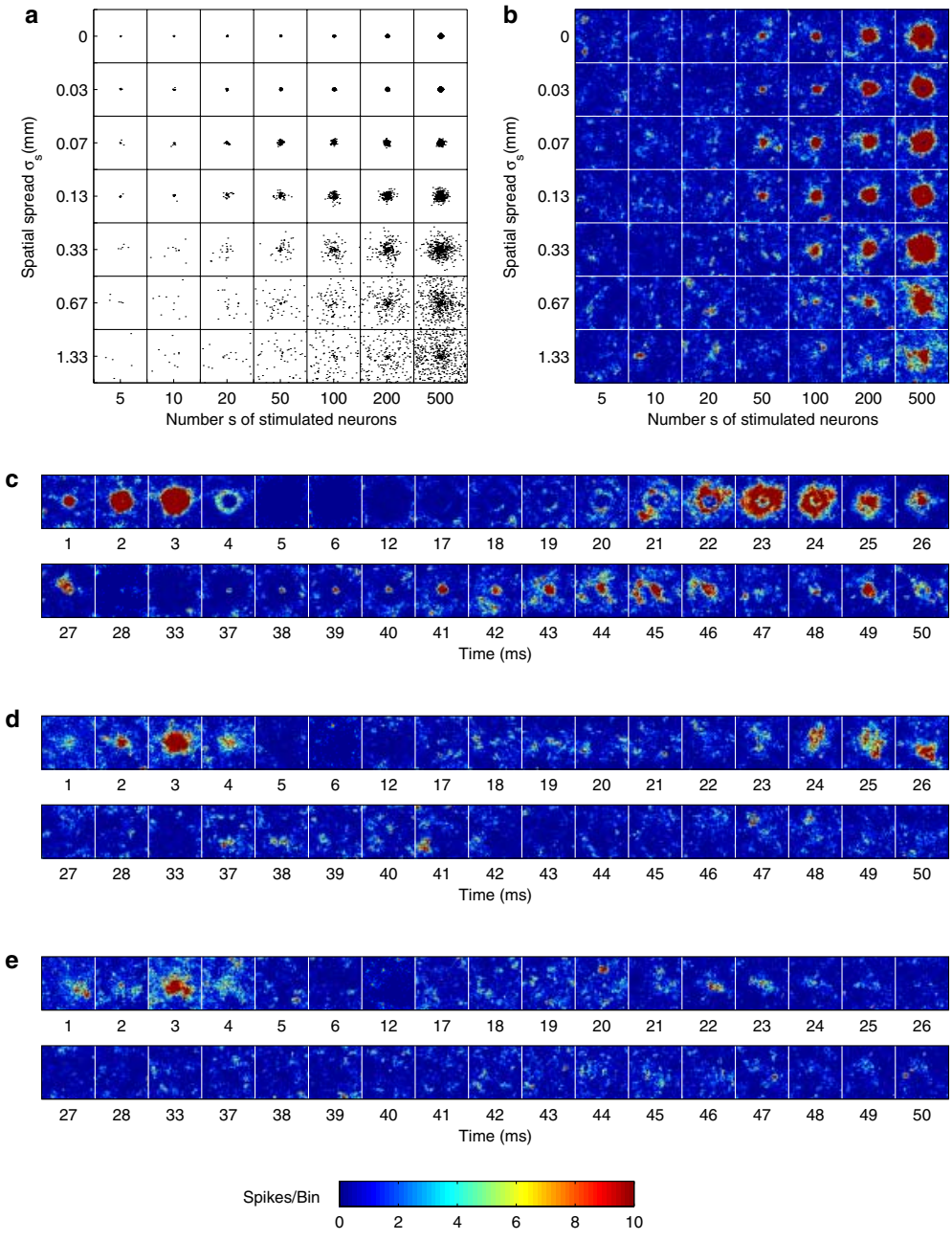

Fig. 5. Network response to a synchronous stimulus of varied strength and spatial spread. In each small square, the spatial axes of 2 mm × 2 mm span the whole network. **a** Locations of stimulated neurons. *Black dots* mark an example of s neurons that are randomly selected with a Gaussian probability of standard deviation σ_s. These neurons are forced to fire a single spike at time 0 and are afterwards subject to reset of membrane potential, refractory period, and synaptic dynamics as if this spike were elicited upon a regular threshold crossing. Stimuli cover the whole range from weak and localized (*upper left*) to strong and diffuse (*lower right*). **b** Network response in the asynchronous-irregular (AI) state with $g = 5.5$, $\nu_{\text{ext}} = 1.9$ (cf. Fig. 2, 3). The stimulus parameters match those in **a**. The color coding shows the number of spikes of the excitatory population, summed in a bin of 5×5 grid points from millisecond 1 to 2, i.e., around one synaptic delay (1.5 ms) after the stimulus. Spikes are pooled from ten repetitions of the stimulus, each time presented after waiting 100 ms for the network to resettle into the stationary AI state. Stimuli of less than $s = 50$ neurons evoke only small center peaks, provided the stimulus is strongly localized (*upper left*). Strong stimuli always elicit an explosion in activity, which is more pronounced and more localized, the more localized the stimulus neurons are. **c** Time evolution of activity explosion. Sample for $s = 500$ and $\sigma_s = 0.13$ mm. Number of repetitions, spatial and temporal bin size as in **b**. The second picture at 2 ms is the same as that in **b** for corresponding s, σ_s. The synfire explosion rapidly recruits neurons in a growing disk that collapses once the effect of the inhibitory explosion takes over (4 ms). An echo of the explosion with a larger temporal spread starts at 17 ms. The second echo at 37ms takes almost 12ms, as compared with only 4 ms for the initial explosion. Later, a third echo has almost dissolved (not shown), the network afterwards resettling into the stationary AI state. **d** Time evolution of activity explosion for $s = 200$, $\sigma_s = 0.67$ mm. The weaker and more diffuse stimulus elicits both an explosion and echoes that are considerably smaller. **e** Time evolution of activity explosion for $s = 200$, $\sigma_s = 1.33$. This even more diffuse stimulus causes only a weak explosion with almost no echoes

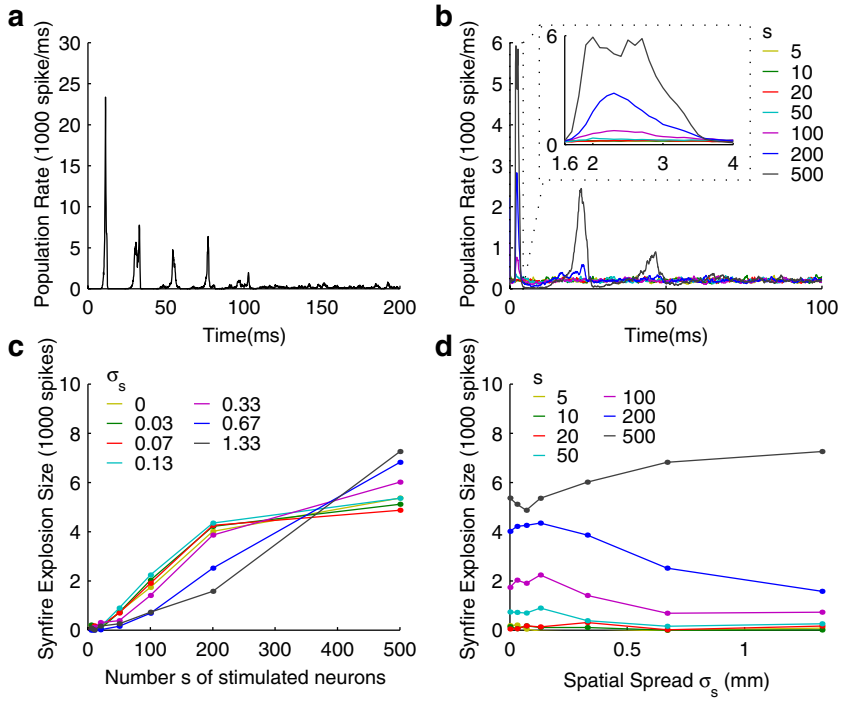

Fig. 6. Strength of synfire explosion and echoes. **a** Initial transient after network initialization. Time trace of population rate during the first 200 ms. The large initial peak causes several echoes before the network settles into a stationary state. **b** Sample averaged population rates for 25 repetitions of a stimulus of fixed spatial spread $\sigma_s = 0.67$ mm and varied strength s as indicated in the legend. The inset shows a zoom into the time interval of the first explosion response from 1.6 ms to 4.0 ms after the stimulus. **c** Average number of spikes fired in response to a stimulus. Stimulus strength s is varied along the abscissa; the colors encode spatial spread σ_s as shown in the legend. The number of spikes in the response activity explosion is calculated as the time integral over the first peak in the averaged population rate (i.e., the inset in **b**). Stimuli with $s = 100$ or more result in a response that is more than ten times stronger. The response saturates when the pool of adjacent neurons is exhausted. Thus, the more diffuse stimuli (*blue* and *black solid curves*) can affect most neurons, but only the strongest one ($s = 500$) manages to fully use this advantage (*black curve*). For lower s, the more localized stimuli (other colors) recruit their lower number of potential target neurons more efficiently. Therefore, both classes intersect ($s \approx 350$). **d** Same data as in **c**, but in dependence of σ_s along the abscissa and color coding for strength s. The response to stimuli of strength $s = 200$ and lower becomes weaker at larger spatial spread. Only the $s = 500$ stimulus (*black curve*) is strong enough to recruit even the large region of its extent. This is the same effect of pool exhaustion and efficiency dependence on localization as described in **c**

3.3 Survival of embedded synfire chains

A synfire chain of width w consists of pools of w neurons each, the groups arranged in sequence and all neurons in a group projecting to all neurons in the next group in a divergent-convergent fashion (Abeles 1991). It was shown that if a sufficient fraction of the neurons in the first group of such a chain fires in synchrony, this spike volley reliably travels down the chain (Diesmann et al. 1999; Gewaltig et al. 2001). Moreover, the all-to-all connectivity of the synfire chain definition can be relaxed to a diluted connectivity if one compensates by either augmenting the intergroup connection strength or by adopting a larger chain width (Hehl et al. 2002). However, these results on the dynamics were obtained for isolated chains, i.e., spikes of the chain neurons did not affect the background activity.

The stimulus investigated in the previous section qualifies as a synfire volley: the stimulated neurons can be understood as the first group of a synfire chain of width s. It was previously shown that in a realistic LCRN at least another s neurons exist with a sufficient multiplicity in connectivity to the first group to qualify as a second synfire group (Hehl et al. 2001; Hehl 2001).

In principle, it should therefore be possible that the spike volley propagates to this second group. As it turned out, however, any such attempt was effectively masked by the synfire explosion: the excitatory population activity involves far more neurons than only the potential second group, and, worse, the overwhelming inhibition in its aftermath quenches any potential propagating spike volley.

To make the synfire connections stronger, we now explicitly embedded a fully connected chain into the network. The mean membrane potential does not differ much from the resting potential. As it takes $w_* = (\Theta - U_r)/J = 147$ simultaneous input spikes to activate a neuron from resting potential to firing threshold, we chose a width that is considerably larger ($w = 250$) in order to obtain a reliable chain (an argument for taking $w \approx 2w_*$ as a choice of width for stable propagation is found in Gewaltig et al. 2001).

There is one remarkable difference in the input a neuron receives in our LCRN and in the isolated chain

case of Diesmann et al. (1999). In the LCRN, a balanced input was obtained by a higher amplitude of the inhibitory than the excitatory PSP, whereas Diesmann et al. (1999) used a higher inhibitory firing rate. As an increased IPSP size results in higher input fluctuations, the distance to firing threshold must be larger if the same neuronal firing rate is desired. Consequently, our group width exceeds the one used by Diesmann et al. (1999), where a width of $w = 100$ was sufficient.

For the embedding, chain neurons were selected as follows. The w neurons of group 1 were drawn at random, obeying a Gaussian probability with standard deviation σ_g. This is the same procedure as was used for the stimulus neurons when investigating the impulse response (Sect. 3.2). For the next group, the center of the Gaussian was moved over a distance d at a random angle, and the neurons of group 2 were drawn in analogous fashion without replacement and all-to-all connected to those of group 1. Iteration of this procedure (for various choices of σ_g and d) was used to construct a chain (Fig. 7a). Clearly, one would prefer a larger network to avoid boundary effects.

Drawing without replacement guarantees that each neuron can be part of the chain in at most one group. On wiring the LCRN, all chain neurons received w fewer excitatory connections to maintain balance. Under these conditions, the length of the chain is limited if one does not want too large a fraction of the network involved in the chain. On the other hand, a long chain is necessary to observe the spike volley propagation. For this reason, we chose a total of ten groups and connected the last group to the first to arrive at a synfire loop.

From the previous section, we already know the strength of the response to a stimulus of $s = w = 250$ simultaneous spikes. Here, we selected parameter settings for σ_g and d that promised qualitatively different results from inspecting the explosion sizes in Fig. 6c,d.

Long simulation times forced us to restrict ourselves to 20 trials for each parameter set, one trial being one realization of the embedding rules stimulated once. The example of the pulse packet propagation in Fig. 7b is representative; variation in qualitative behavior across trials was low. Observe that there are two modes of pulse propagation. One relies on small groups that elicit localized explosions, the next group being situated far enough to not be extinguished by this explosion (e.g., $\sigma_g = 0.17$ mm, $d = 0.5$ mm or $d = 1.33$ mm, compare Fig. 7c,d). In the other mode, neurons in each group are spread wide enough to restrict the explosion such that the synfire volley may survive, even if it cannot escape ($\sigma_g = 0.67$ mm, $d = 1.33$ mm). For all other parameter sets, the volley sooner or later dies out, with few exceptional trials where it survived over the observation time window.

Even those parameter values for which the volley propagates do not show a sharp synchronization along the chain, and the temporal jitter changes from group to group in an unpredictable manner. At the same time, network activity is not particularly reliable. On the contrary, the chain may be ignited spontaneously by the initial transient (Fig. 6a), with the network never reaching an AI state where the stimulus could meaningfully be applied. Alternatively, the explosion elicited by group i may stimulate other groups besides $i + 1$, leading to multiple volleys propagating in the chain that interfere with each other. The echo of an explosion may have the same effect, all this leaving groups in a refractory state when the "regular" volley arrives, which is then bound to perish.

In summary, under the conditions studied it is indeed possible to adjust parameters to obtain an embedded chain that sustains synfire activity. But this is neither the natural mode in the sense that many such physiologically plausible parameter settings would exist, nor is the synfire propagation reliable such that one could predict the time and shape of the volley at a given group. Moreover, the chain dynamics dominate the entire network dynamics, kicking them out of the AI state.

4 Discussion

Motivated by the anatomical findings that on a local scale neocortical neurons are connected with a Gaussian probability, we explored the activity dynamics of a locally connected random network (LCRN) of about 10^5 neurons using simulations. By adjustment of inhibitory weight and strength of external input, this network settles in a dynamical state of asynchronous network activity and irregular single-neuron spiking, similar to the AI state of sparsely connected random networks (Brunel 2000; Amit and Brunel 1997). However, in these studies it is assumed that no correlations exist between neurons beyond a common time-varying rate. For an LCRN we demonstrated correlations in the spike patterns of adjacent neurons even in the AI state. The correlations remain with increasing network size as this leaves the number of synapses and the spatial localization of the connectivity unaffected. As a consequence of this network scaling, the phase diagram of the dynamical states of a sufficiently large LCRN (Fig. 2) is independent of the network size and is a result of the network parameters chosen in accordance with anatomy. A network size of about 10^5 neurons for the first time allows us to investigate networks with a realistic connectivity rule and a realistic number of synapses per neuron. Therefore, our parameters have an absolute meaning, and it is pointless to discuss the scaling behavior of observed effects with increasing network size. A minimal network size is required to avoid boundary effects, and a sheet of 2×2 mm proved sufficient to not influence the network states in our study.

For an LCRN in the AI state, sharp spike correlations rapidly drop to zero for distances between neurons of more than 0.5 mm. This is in agreement with experimental findings in the cortex of awake monkeys, where sharp correlations were found for adjacent neurons, but not any longer if these neurons were more than 0.5 mm apart (e.g., Vaadia and Aertsen 1992). Therefore, we consider the activity of the LCRN in the AI state as a more realistic model of cortical background activity than uncorrelated noise.

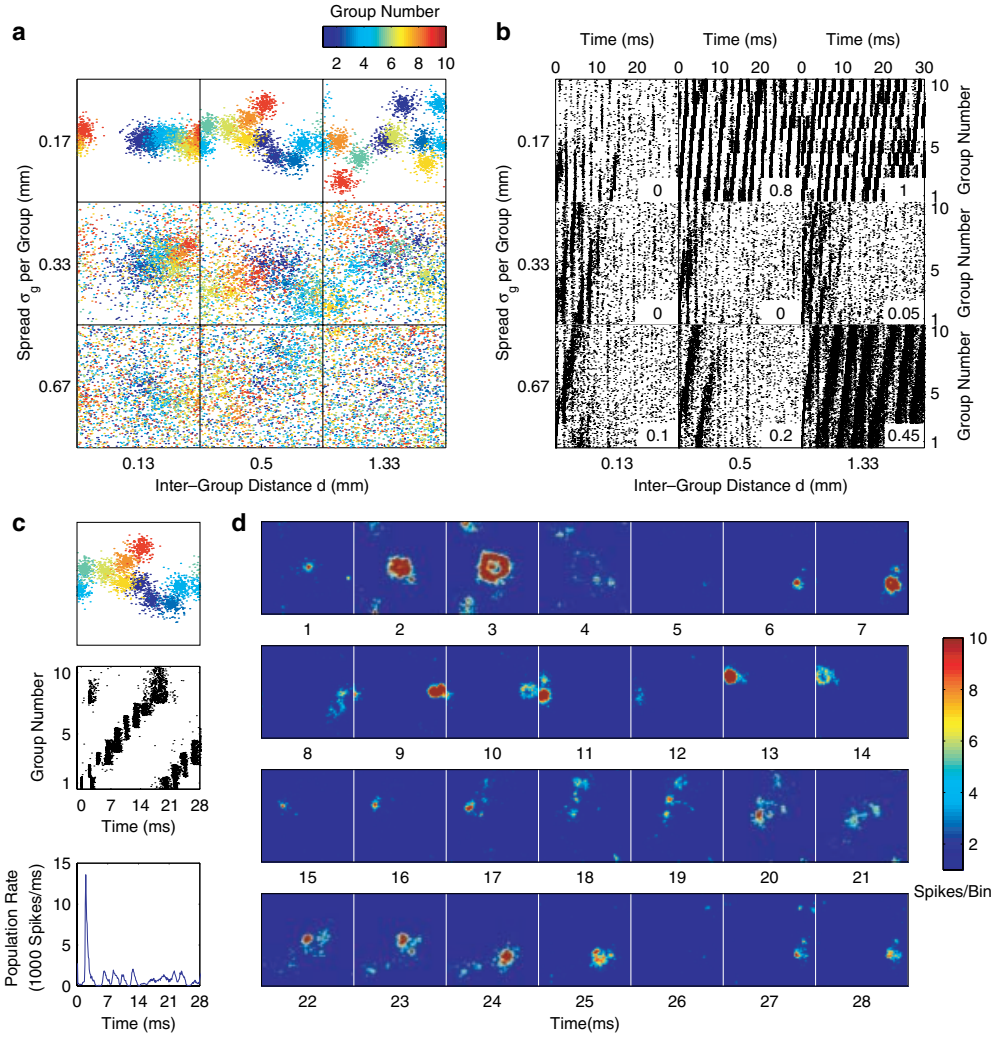

Fig. 7. Dynamics of an embedded synfire chain. **a** Synfire chain embedding scheme. Neurons in each group ($w = 250$) are selected at random according to a Gaussian profile with standard deviation σ_g, depending on the distance to the group center. From group to group, this center roams in a random direction (uniform random angle between 0 and π vs. negative y-axis, forcing a drift to the right) with step size d. Colors encode the group number. The tenth and last group (red) is connected to the first (blue), establishing a synfire loop. Group spread and intergroup distance were varied systematically, as indicated by the matrix. **b** Activity of the synfire chain. Each panel corresponds to the embedding parameters of **a**. At time 0, all neurons of the first group are forced to spike. Panels show the time evolution of spiking activity of the 2,500 chain neurons (neurons sorted at the ordinate according to the group they belong to). In these sample responses to a single stimulus each, only a fraction of synfire loops propagate the synchronous spike volley (*upper middle*, *right*, and *lower right*). Moreover, the larger the spatial spread in a single group, the larger the temporal dispersion of the response spikes (compare, e.g., *upper right* and *lower right*). The probability for a loop to propagate activity, obtained from 20 different realizations of embedding with identical parameters, is indicated in the *lower right* of each panel. **c** Details for a single sample synfire chain. The *upper* panel shows the embedding scheme (same as *upper middle* in **a**); the *middle* panel presents a close-up of the first 28 ms after stimulus. The first group fires not only the forced stimulus spikes, but again after about 3 ms. Propagation of the spike volley along the chain is not reliable; the strong synchronicity of the initial stimulus gets lost. The *lower* panel shows the overall excitatory population rate for this time interval. The response to the initial stimulus is by far the most pronounced, but all groups trigger response explosions. **d** Network activity as a spike volley propagates along an embedded chain. The same sample is taken as in **c**, the binning along spatial coordinates as in Fig. 5. The volley traveling along the chain can be visually tracked by the explosions elicited with a delay of a few milliseconds (compare with the embedding scheme and the group's activity in **c**). The initial stimulus results in a strong activity explosion (1–3 ms). After 2 ms, the second group is already active, overshadowed by the explosion. This process repeats along the chain: a small activity spot for the volley, followed by a larger explosion. After 22 ms, the pulse arrives again at group 1, starting the second cycle

When an excitatory stimulus of varying spatial spread and number of affected neurons is applied to the network, it responds with an explosion in activity that is afterwards quenched when the inhibitory spikes in the explosion cut the excitability. Since this is exactly the kind of stimulus that a synchronous spike volley traveling along a synfire chain would emit, we explicitly embedded such a subnetwork into the LCRN. We found that the synfire explosion prohibits reliable pulse propagation in a synfire chain. Even though by proper choice of embedding parameters it is indeed possible to sustain synfire activity, the timing precision within a pulse packet does not remain constant, nor is its arrival time predictable. This result is in clear contrast to the

simple attractor characteristics in the state space of an isolated chain (Diesmann et al. 1999).

Previously it was predicted that the connectivity in an LCRN would suffice to inherently provide for the connections that establish a diluted synfire chain, i.e., a chain where the requirement of all-to-all connectivity within the chain is relaxed (Hehl et al. 2001). Although these structures are indeed present, the spacing of subsequent group centers in that case is much closer than in our explicit embedding procedure (0.03 mm intergroup center distance in the inherent chain, compared to the minimal value of 0.13 mm in Fig. 7). Since the fully connected embedded chain does not appear to support stable spike volley propagation, an inherent diluted chain is even less likely to do so.

A shortcoming of our simulations are the remainders of boundary effects due to the finite network size. These, however, are not to be held responsible for the synfire explosion, which, as we will see in a moment, is a general feature of the network dynamics. Nevertheless, activity in the embedded chain could more easily survive if subsequent groups were located in parts of the network that were untouched by its previous activity.

We now want to put forth the argument that the synfire explosion is a robust phenomenon found in a large class of networks. Consider a network where all neurons are connected randomly at a fixed percentage, say $c = 0.1$. The instantaneous membrane potential distribution of these neurons, as they are many, will be near to a Gaussian. We assume that an estimate for the number of neurons activated by a stimulus is determined by that part of the Gaussian that is near enough to the firing threshold to cross it one synaptic delay later (for related concepts see Abeles 1982; Boven and Aertsen 1990; Abeles 1991).

This procedure is illustrated by the membrane potential distribution of our LCRN in the AI state, together with a Gaussian fit (Fig. 8a). The complete distribution is skewed, as the weight of an inhibitory PSP is stronger by a factor g compared to the excitatory PSPs. Additionally, our model does not include any reversal potentials that would cut off low membrane potential values and thereby reduce the skewness. As we are interested in the membrane potential distribution near the firing threshold, we circumvent problems introduced by this skewness by only considering the falling edge close to threshold.

An excitatory stimulus from s additional spiking neurons will, in the mean, add an amount of $d = c \times s \times J$ to an individual neuron's membrane potential. Therefore, the number of neurons activated by this stimulus is determined as the integral of the membrane potential distribution calculated over the range $[\Theta - d, \Theta]$. The additional spikes thus elicited are shown in dependence of s (Fig. 8b). Qualitatively, this simple model already explains the synfire explosion in Fig. 6c. There, in the LCRN case, the explosive effect saturates for large s, because the pool of neighboring neurons is limited, and these are the ones affected by the stimulus. In summary, even though there may be quantitative

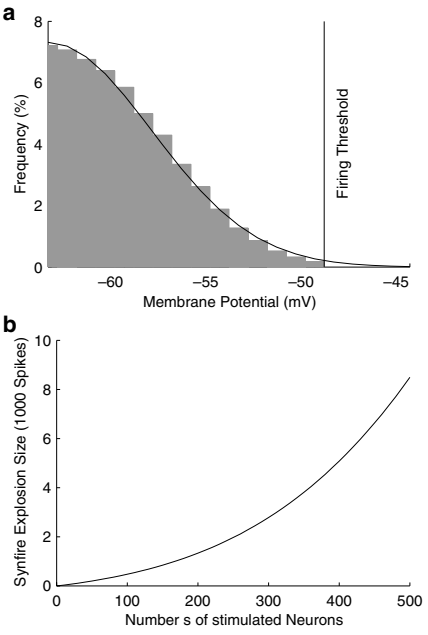

Fig. 8. Gaussian model to illustrate universality of the synfire explosion. **a** The model for a simple network architecture. The membrane potential distribution (*gray area*) taken from 100 neurons traced over 400 ms of simulated time is approximated by a Gaussian with $\mu = -63.00$ mV and $\sigma = 5.45$ mV (nonlinear Levenberg-Marquardt fit (Press et al. 1992)). Neurons with membrane potential larger than the firing threshold of 50 mV are assumed to fire an action potential. **b** Number of spikes elicited in a simple network of 90,000 neurons with constant connectivity $c = 0.1$. As the number of stimulating neurons s is increased, the response spike number grows supralinearly: the gain factor rapidly rises above 1, reaching nearly 20 for $s = 500$ stimulated neurons

differences in the severity of the explosion, it appears to be a universal feature.

In a random network, however, the effect of a fixed number of neurons, as in this explosion, is negligible as compared to background activity once the network size is sufficiently large. Consequently, the inhibitory explosion is smaller and more diffuse and will not quench all activity in the aftermath. By contrast, increasing the size of the LCRN preserves the neighborhood coupling and therefore the effect of the explosion.

It could be argued that our results are an artifact of homogeneity assumptions that entered the model. We decided on having the connectivity space constant for excitatory and inhibitory neurons the same as a forced guess, due to a lack of quantitative anatomical data. Different connectivity ranges of the excitation and the inhibition can lead to different patterns of activity (Wilson and Cowan 1973; Ermentrout and Cowan 1979a,b). Therefore, we could expect to find different phase diagrams in these cases, but we assume an AI state to still exist. The synfire explosion, being an effect of the excitatory-excitatory connections alone, should not be affected.

In addition, to obtain more heterogenous networks, one could introduce varying individual firing thresholds, synaptic strengths, conduction delays, or membrane time constants. Random networks have been shown to

exhibit an AI state in spite of a varying threshold (van Vreeswijk and Sompolinsky 1996) and varying conduction delays (Brunel 2000). It seems unlikely, therefore, that any of the variations mentioned is a candidate to cause fundamental changes in the qualitative behavior of our network model, as long as it can be assumed that all the parameters listed could still be described by a mean and a variation that preserve the order of magnitude. We can divide the properties that might be subject to variations into two classes, one that describes the likelihood that the neuron will fire in dependence of the number of inputs (firing threshold, synaptic strength), the other concerned with temporal integration (conduction delay, membrane time constant). The variations in the likelihood to fire will average out and not have a large impact on the size of the synfire explosion (cf. model in Fig. 8). The temporal integration properties would only change the time scale of the synfire explosion. Figure 7 demonstrates that the pulse packet traveling along the chain causes a synfire explosion in spite of a time jitter of at least 1 ms. Realistic variations in the conduction delays are in that regime. As long as the temporal jitter in the stimulating neurons is smaller than the rise time of the PSP, different membrane constants essentially do not play a role: PSP time traces are very similar up to the peak for a wide range of membrane time constants (5–20 ms).

We do not, on the other hand, claim that all dynamic states in Fig. 2 are unaffected; for instance, the synchronous states might vanish. But homogeneity should rather disfavor the AI state, the one that is crucial for our investigation, though the exact shape of the AI regime surely will vary. We conclude that the existence of the AI state and the emergence of the synfire explosion are not due to homogeneity.

The size of the synfire explosion, however, depends on the required width of the synfire chain. Both the synaptic strength within the chain and the distance from firing threshold to mean membrane potential will affect this required width. This suggests that it might be possible, after properly adjusting these parameters, to prohibit the occurrence of an activity explosion. However, as the dependence of the required width on both parameters is almost linear and the regime of plausible values is restricted, such variation results in a reduction to half the required width at best. These more than 100 neurons per group will still elicit an explosion in the order of 1000 activated neurons (Fig. 6c), demonstrating that adjusting synaptic strength is no way out.

Then how could a synfire chain cope with this activity explosion? The simplest answer would be to conclude that synfire groups are not local but spread over a large cortical area, thereby avoiding an explosion. This may be correct from a dynamics point of view, but anatomical considerations indicate that nonlocal synfire groups are unlikely for a statistical lack of sufficient multiplicity in intergroup connectivity (Hehl et al. 2001; Hehl 2001).

It is conceivable that by careful tuning of network parameters the propagation in a single chain could be made more reliable. An alternative solution would be that the fine structure of the cortical network deviates from that of a random graph in that it is organized to avoid the malicious intermediate convergence levels of neurons receiving input from a synfire group. This would naturally prevent a synfire explosion. A possible justification for such a scheme would be given if the synfire chain were the result of an appropriate kind of learning process. Whether such network structures are compatible with stability conditions and experimentally observed membrane potential statistics remains to be investigated. In any case, adopting such modifications would appear to violate the universality of the synfire scheme. Another option would be to include long-range patchy connectivity, either within the same area (Amir et al. 1993) or across areas (Schüz and Liewald 2001), to relax the locality constraints, but not enough anatomical data are currently available to judge the biological feasibility of this option.

The more attractive and promising solution would be to include inhibitory neurons into the chain (Fig. 9). A similar proposal was made by Hayon et al. (1999) but for a different purpose: to regulate the level of binding between multiple synfire chains. These inhibitory cells are activated by the propagating spike volley, their influence weakening or even preventing the synfire explo-

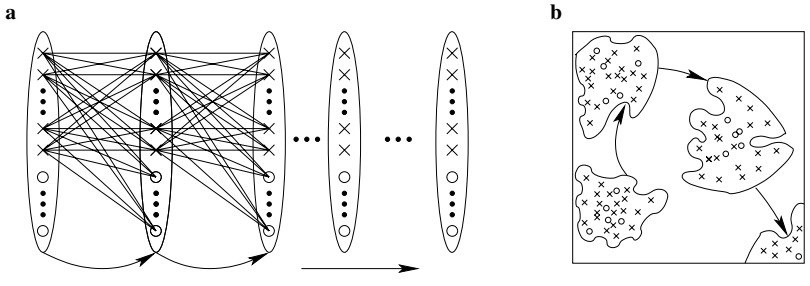

Fig. 9. Scheme of a generalized synfire chain. **a** Connectivity of the chain (see also Hayon et al. (1999)). Each synfire group includes not only excitatory neurons (marked as"x"), but also inhibitory ones ("o"), e.g., one fourth their number to suit the overall population sizes. The excitatory group neurons are completely connected in divergent-convergent fashion as in the original definition. Additionally, all excitatory neurons project to all inhibitory neurons of the succeeding group, but these inhibitory neurons in turn do not establish any specific chain connections. **b** Spatial embedding of the chain. The excitatory neurons of the chain are distributed as in the embedded chain simulations (see Fig. 7a), but in addition, inhibitory neurons are interspersed

sion, while they do not specifically target the succeeding group, which would terminate the pulse propagation. Preliminary results indeed show that the explosive impulse response to a simultaneous excitatory and inhibitory stimulus in this case is at least less pronounced, if it occurs at all.

Previous studies computed capacity limits, specifying how many synfire groups can be sustained in a network of a certain size (Bienenstock 1995; Herrmann et al. 1995). Both studies artificially introduced an inhibitory mechanism alongside the synfire activity. In the case of Bienenstock (1995), population activity was bounded by a *d*-winner-take-all neuron model, whereas Herrmann et al. (1995) tied an ad hoc global inhibition term to the synfire activity to restrict overall activity. These types of inhibition presumably prevent an activity explosion. It is obvious that these capacity computations cannot be applied straightforwardly to our LCRN: with the model as presented, the capacity does not even suffice to sustain ten groups, several orders of magnitude less than the capacities cited. An inclusion of inhibition into the chain could possibly be made compatible with these capacity estimates.

For the synfire hypothesis to survive, it is vital to stabilize the pulse packet propagation against the synfire explosion. Moreover, multiple interacting chains should not even locally dominate the network activity, as it is hard to imagine that so many neurons would be "invested" in the survival of only a few stable synfire chains. Indeed, more insight into the dynamics of realistic neural network models is urgently needed to reach a decision on the biological viability of the synfire scheme.

Acknowledgements. Stimulating discussions with Stefan Rotter and Moshe Abeles are gratefully acknowledged. We thank Denny Fliegner for setting up the parallel computing facilities at the MPI für Strömungsforschung, which was used for part of the simulations. Partial funding was received from the Boehringer Ingelheim Fonds, the Deutsche Forschungsgemeinschaft (DFG Ae 10/3), the Human Frontier Science Program (HFSP), and the German-Israeli Foundation for Research and Development (GIF).

References

Abeles M (1982) Local cortical circuits: an electrophysiological study. Studies of brain function. Springer, Berlin Heidelberg New York

Abeles M (1991) Corticonics: neural circuits of the cerebral cortex. 1st edn, Cambridge University Press

Amari Si (1977) Dynamics of pattern formation in lateral-inhibition type neural fields. Biol Cybern 27: 77–87

Amir Y, Harel M, Malach R (1993) Cortical hierarchy reflected in the organization of intrinsic connections in macaque monkey visual cortex. J Comp Neurol 334: 19–46

Amit DJ, Brunel N (1997) Model of global spontaneous activity and local structured activity during delay periods in the cerebral cortex. Cereb Cort 7: 237–252

Arieli A, Sterkin A, Grinvald A, Aertsen A (1996) Dynamics of ongoing activity: explanation of the large variability in evoked cortical responses. Science 273: 1868–1871

Bienenstock E (1995) A model of neocortex. Netw Comput Neural Sys 6: 179–224

Boven KH, Aertsen A (1990) Dynamics of activity in neuronal networks give rise to fast modulations of functional connectivity. In: Eckmiller R, Hartmann G, Hauske G (eds) Parallel processing in neural systems and computers. Elsevier, Amsterdam, pp 53–56

Braitenberg V, Schüz A (1998) Cortex: statistics and geometry of neuronal connectivity, 2nd edn. Springer, Berlin Heidelberg New York

Brunel N (2000) Dynamics of sparsely connected networks of excitatory and inhibitory spiking neurons. J Comput Neurosci 8: 183–208

Diesmann M, Gewaltig MO (2002) NEST: An environment for neural systems simulations. In: Macho V (ed) Forschung und wissenschaftliches Rechnen, GWDG-Bericht, Gesellschaft für wissenschaftliche Datenverarbeitung, Göttingen

Diesmann M, Gewaltig MO, Aertsen A (1995) SYNOD: an environment for neural sytems simulations. Language interface and tutorial. Tech Rep GC-AA-/95-3, Grodetsky Center for Research of Higher Brain Functions, Weizmann Institute of Science, Israel

Diesmann M, Gewaltig MO, Aertsen A (1999) Stable propagation of synchronous spiking in cortical neural networks. Nature 402: 529–533

Diesmann M, Gewaltig MO, Rotter S, Aertsen A (2001) State space analysis of synchronous spiking in cortical neural networks. Neurocomputing 38–40: 565–571

Ermentrout GB, Cowan JD (1979a) A mathematical theory of visual hallucination patterns. Biol Cybern 34: 137–150

Ermentrout GB, Cowan JD (1979b) Temporal oscillations in neuronal nets. J Math Biol 7: 265–280

Gabbott P, Stewart M (1987) Distribution of neurons and glia in the visual cortex (area 17) of the adult albino rat: a quantitative description. Neuroscience 21: 833–845

Gewaltig MO, Diesmann M, Aertsen A (2001) Propagation of cortical synfire activity: survival probability in single trials and stability in the mean. Neural Netw 14: 657–673

Hayon G, Abeles M, Lehmann D (1999) Part binding in a noisy environment by dynamic binding of synfire chains. In: NTCS 99: Computationalism, the next generation, University of Vienna, Austria, pp 70–79

Hehl U (2001) Embedding of synchronous spike activity in cortical networks. Ph.D. thesis, Fakultät für Biologie, Albert-Ludwigs-Universität Freiburg

Hehl U, Aertsen A, Diesmann M (2002) Dynamics of diluted synfire chains. Biol Cybern, submitted

Hehl U, Hellwig B, Rotter S, Diesmann M, Aertsen A (2001) Localization of synchronous spiking as a result of anatomical connectivity. Soc Neurosci Abstr 27: 64.1

Hellwig B (2000) A quantitative analysis of the local connectivity between pyramidal neurons in layers 2/3 of the rat visual cortex. Biol Cybern 82: 111–121

Herrmann M, Hertz JA, Prügel-Bennett A (1995) Analysis of synfire chains. Network 6: 403–414

Krone G, Mallot H, Palm G, Schüz A (1986) Spatiotemporal receptive fields: a dynamical model derived from cortical architectonics. Proc R Soc Lond B 226: 421–444

Pacheco PS (1997) Parallel programming with MPI. Morgan Kaufmann, California

Peters A, Kara DA, Harriman KM (1985) The neuronal composition of area 17 of rat visual cortex. III. Numerical considerations. J Compar Neurol 238: 263–274

Press WH, Teukolsky SA, Vetterling WT, Flannery BP (1992) Numerical recipes in C, 2nd edn. Cambridge University Press

Rotter S, Diesmann M (1999) Exact digital simulation of time-invariant linear systems with applications to neuronal modeling. Biol Cybern 81: 381–402

Schüz A, Liewald D (2001) Patterns of cortico-cortical connections in the mouse. In: Proceedings of the 28th Göttingen Neurobiology Conference, Thieme, Stuttgart, p 624

Tuckwell HC (1988) Introduction to theoretical neurobiology, vol 1. Cambridge University Press

Vaadia E, Aertsen A (1992) Coding and computation in the cortex: single-neuron activity and cooperative phenomena. In: Aertsen A, Braitenberg V (eds) Information processing in the cortex. Springer, Berlin Heidelberg New York, pp 81–121

Van Vreeswijk C, Sompolinsky H (1996) Chaos in neuronal networks with balanced excitatory and inhibitory activity. Science 274: 1724–1726

Van Vreeswijk C, Sompolinsky H (1998) Chaotic balanced state in a model of cortical circuits. Neural Comput 10: 1321–1371

Wilson HR, Cowan JD (1973) A mathematical theory of the functional dynamics of cortical and thalamic nervous tissue. Kybernetik 13: 55–80